Soil reinforcement through addition and subsequent carbonation of wollasonite microfibres

S. Pourakbar[1], M. H. Fasihnikoutalab[2], R. J. Ball[3], N. Cristelo[4] and B. K. Huat[5]

[1] *PhD, Assistant professor, Department of Civil Engineering, Faculty of Engineering, University of Binaloud, Moallem street, Mashhad, Iran, E-mail: pourakbar@binaloud.ac.ir*
[2] *PhD, Assistant Professor, Department of Civil Engineering, Faculty of Engineering, University Putra Malaysia, 43400 Serdang, Selangor Darul Ehsan, Malaysia, E-mail: hfasih@gmail.com (corresponding author)*
[3] *PhD, Reader, BRE Centre for Innovative Construction Materials, Department of Architecture and Civil Engineering, University of Bath, Bath, UK, E-mail: r.j.ball@bath.ac.uk*
[4] *PhD, Assistant professor, CQ-VR, Centro de Química – Vila Real, Department of Engineering, University of Trás-os-Montes e Alto Douro, Apartado 1013, 5001-801 Vila Real, Portugal, E-mail: ncristel@utad.pt*
[5] *Professor, Department of Civil Engineering, Faculty of Engineering, University Putra Malaysia, 43400 Serdang, Selangor Darul Ehsan, Malaysia, E-mail: dean.sgs@upm.my*

Received 10 January 2017, revised 30 April 2017, accepted 30 June 2017, published 15 November 2017

ABSTRACT: This study describes the application of wollasonite microfibres for stabilising soil with the additional function of sequestering CO_2. The high aspect ratio, needle-like structure of wollasonite imparted a microfibre mechanical reinforcement whilst the associated high surface area promoted carbonation. The originality of this paper lies in two unique aspects: the first stage assessed the efficacy of incorporating wollastonite microfibres inside the soil mass, while the second stage addressed the mechanical performance of the fibre-reinforced soil after different CO_2 pressures and carbonation times. In these two stages, the unconfined compressive strength (UCS), indirect tensile strength (ITS) and flexural strength (FS) were determined. The test results indicated that the inclusion of the fibres increased the peak and post-peak response during unconfined compressive strength (UCS) tests, while also improving the ITS and FS. The UCS peak stress was further improved when the fibre-reinforced soil was subjected to the carbonation process. This work impacts the soil stabilisation industry through a novel soil strengthening process that also promises an effective route to combat climate change through sequestration of CO_2.

KEYWORDS: Geosynthetics, Soil reinforcement, Wollastonite microfibres, Ground improvement, Carbonation process

REFERENCE: Pourakbar, S., Fasihnikoutalab, M. H., Ball, R. J., Cristelo, N. and Huat, B. K. (2017). Soil reinforcement through addition and subsequent carbonation of wollasonite microfibres. *Geosynthetics International*, **24**, No. 6, 554–564. [http://dx.doi.org/10.1680/jgein.17.00021]

1. INTRODUCTION

Discrete fibre reinforcement is one of the physical methods of soil improvement, in which the strength of the original soil is enhanced by the addition of a reinforcing agent with high tensile strength (Tang *et al*. 2007; Consoli *et al*. 2012; Estabragh *et al*. 2012; Fatahi *et al*. 2012; Hejazi *et al*. 2012; Correia *et al*. 2015; Cristelo *et al*. 2015, 2017). Among different reinforcing possibilities, fibres represent a very interesting option for engineering applications, mainly due to their adaptability to conventional mixing techniques and low cost of fabrication (Lin *et al*. 2010; Botero *et al*. 2015; Pourakbar and Huat 2016, 2017).

A significant amount of research has been conducted to assess the effectiveness of various types of fibres, such as jute (Aggarwal and Sharma 2011; Singh and Bagra 2013; Güllü and Khudir 2014), coir (Sivakumar Babu and Vasudevan 2008; Ramesh *et al*. 2010; Maliakal and Thiyyakkandi 2013), sisal (Prabakar and Sridhar 2002), bamboo (Thwe and Liao 2002), palm fibre (Marandi *et al*. 2008), polyethylene fibre (Tang *et al*. 2007; Sukontasukkul and Jamsawang 2012; Botero *et al*. 2015; Cristelo *et al*. 2015), carpet waste fibre (Mirzababaei *et al*. 2012) and glass fibre (Yeung *et al*. 2007). Review of the literature validates the proposition that, although there are numerous types of fibre available with the potential for use as reinforcement to improve certain engineering properties of soil, research has focused on a small number of different types of man-made and natural fibres.

This study focused on mineral wollastonite microfibres due to their ability to enhance the mechanical properties

of soils, coupled with the ability to sequester carbon dioxide, by carbonation. Wollastonite is an inosilicate mineral, composed essentially by calcium silicate ($CaSiO_3$), thus possessing very significant percentages of calcium (40–50%) and silica (40–55%). It is formed in nature by the interaction of silica (SiO_2) and calcite ($CaCO_3$), and the subsequent loss of carbon dioxide, under high pressure and temperature (Saltevskaya *et al.* 1974).

One of wollastonite's most unusual characteristics is its high aspect ratio needle-like structure, which increases its effectiveness as a reinforcing fibre (Low and Beaudoin 1993, 1994a, 1994b; Kalla *et al.* 2013; Dey *et al.* 2015; Pourakbar *et al.* 2016; Pourakbar and Huat 2017). Besides, in the current global marketplace, the price of wollastonite ranges from US$0.2 to 0.3/kg, depending on its size (Soliman and Nehdi 2011), which is significantly lower than the price of steel fibres – US$6.6/kg (Ding *et al.* 2011), carbon fibres – US$11.0/kg, or glass fibres – US $2/kg (Clark 1998).

Recent evidence suggests the high potential of wollastonite for direct carbonation (Tai *et al.* 2006; Daval *et al.* 2009). It is widely accepted that minerals such as olivine, wollastonite, and serpentine are particularly suitable for carbon dioxide sequestration, which results in decreasing CO_2 levels in the atmosphere (Fasihnikoutalab 2015; Ashraf *et al.* 2016; Fasihnikoutalab *et al.* 2016a, 2017a, 2017b). In this respect, Ca silicates like wollastonite tend to be more reactive towards carbonation compared to Mg silicates such as olivine (Lackner *et al.* 1997). Regarding the wollastonite mineral, which is particularly suited for CO_2 sequestration due to the high reactivity of its Ca silicates, the overall weathering reaction can be written as shown in Equation 1 (Huijgen *et al.* 2006).

$$CaSiO_{3(S)} + CO_{2(g)} \rightarrow CaCO_{3(S)} + SiO_{2(g)} \quad (1)$$

There are several industrial techniques utilising minerals for CO_2 sequestration. The most promising of these techniques is known as 'aqueous carbonation', consisting of a gas-solid-water slurry mixing, more effective than the more direct gas-solid approach (O'Connor *et al.* 2005). According to previous studies, the aqueous carbonation of wollastonite occurs in three steps, namely the leaching of the Ca (Equation 2), then the dissolution of the CO_2, followed by the conversion of the carbonate species (Equation 3); and finally the nucleation of the calcium carbonate (Equation 4) (Huijgen *et al.* 2006; Andreani *et al.* 2009; Prigiobbe *et al.* 2009; Zhao *et al.* 2009; Ashraf *et al.* 2016).

$$CaSiO_3 + 2H^+ \rightarrow Ca^{2+} + H_2O + SiO_2 \quad \text{Leaching} \quad (2)$$

$$CO_2 + H_2O \rightarrow H_2CO_3 \rightarrow HCO_3^- + H^+ \quad \text{Dissolution} \quad (3)$$

$$Ca^{2+} + HCO_3^- \rightarrow CaCO_3 + H^+ \quad \text{Nucleation} \quad (4)$$

Huijgen *et al.* (2006) investigated the mechanisms of aqueous wollastonite carbonation as a possible carbon dioxide sequestration process by systematically changing the reaction temperature, CO_2 pressure, particle size, reaction time, liquid to solid ratio, and intensity of agitation. According to this study, the carbonation was observed to occur via two sequential processes: (1) Ca leaching from the $CaSiO_3$ matrix and (2) $CaCO_3$ nucleation and growth. Moreover, and according to Ashraf *et al.* (2016), the carbonation reaction of wollastonite forms two main products: calcium carbonate ($CaCO_3$) and an amorphous silica gel (SiO_2). According to this investigation, the effective elastic moduli of carbonated wollastonite pastes are levelled with the values obtained for hydrated high to ultra-high performance cement pastes.

The present study investigates the effectiveness of wollastonite microfibres, before and after carbonation, for soil stabilisation. In the first stage of this research, wollastonite microfibres were incorporated into the soil in the form of an evenly dispersed discrete reinforcement. In the second stage, carbonation of the already reinforced soil was performed, using gaseous CO_2, injected for different periods at different pressures. Two types of test were carried out before and after carbonation, to characterise the compressive (using the uniaxial compression strength test) and tensile strength (using the indirect tensile strength and flexural strength tests). Results were further elaborated through the investigation of microstructural changes.

2. MATERIALS AND METHODS

2.1. Materials

The physical properties and chemical composition of the clayey soil used in this experiment are listed in Tables 1 and 2, respectively. It is noteworthy that, according to the Unified Soil Classification System (ASTM D2487),

Table 1. Physical characteristics of clayey soil

Basic soil property	Standard	Value
Specific gravity	BS 1377: Part 2	2.6
Liquid limit (%)	BS 1377: Part 2	60.24
Plastic limit (%)	BS 1377: Part 2	30.11
Optimum moisture content (OMC) (%)	BS 1377: Part 4	32
Maximum dry density (MDD) (Mg/m^3)	BS 1377: Part 4	1.29

Table 2. Chemical composition of natural soil and wollastonite microfibres

Constituent	Natural soil (%)	Microfibre (%)
Silica (SiO_2)	30.98	40–55
Alumina (Al_2O_3)	18.35	< 1
Iron oxide (Fe_2O_3)	12.8	< 1
Calcium oxide (CaO)	0.2	40–50
Potash (K_2O)	6.67	< 1
Magnesia (MgO)	0.5	< 5
Loss on ignition	—	< 5

Table 3. Mixture proportions of various series of specimens for UCS, ITS and FS tests

Group series	Test no.	OMC (%)	MDD (Mg/m^3)	UCS	Flexural strength (FS) Indirect tensile strength (ITS)
S group	S	32	1.356	7, 14, 28 d	28 d
W_BS group	$W_{10\%}$S	25.1	1.386	7, 14, 28 d	28 d
	$W_{15\%}$S	23	1.53	7, 14, 28 d	28 d
	$W_{20\%}$S	20	1.72	7, 14, 28 d	28 d
Carbonated group	$S_{(200,24)}$	—	—	200 kPa, 24 h	200 kPa, 24 h
	$C_{(100,12)}W_{20\%}$	—	—	100 kPa, 12 h	100 kPa, 12 h
	$C_{(100,24)}W_{20\%}$	—	—	100 kPa, 24 h	100 kPa, 24 h
	$C_{(200,12)}W_{20\%}$	—	—	200 kPa, 12 h	200 kPa, 12 h
	$C_{(200,24)}W_{20\%}$	—	—	200 kPa, 24 h	200 kPa, 24 h

the original soil is classified as high-plasticity clay (CH). The mechanical behaviour of this type of soil is often found to be unacceptable for many structural applications, thus requiring on-site stabilisation. Commercially available mineral wollastonite microfibres were added to the soil, in percentages of 10, 15, and 20% by dry weight of soil. Table 2 presents some of the chemical characteristics of the microfibres, as provided by the manufacturer.

2.2. Laboratory tests

2.2.1. *Mixing procedure*

To obtain a uniform distribution of the microfibres within the soil, different mixing procedures were investigated to identify the most effective method. These included mixing prewetted microfibres with dry soil powder, mixing dry microfibres with wet soil, and mixing dry soil and microfibres followed by the addition of distilled water. It was observed that the most suitable mixing procedure was obtained when distilled water was added to a dry combination of microfibres and soil. This mixing procedure resulted in less agglomeration of the microfibres, because microfibres were first coated with a layer of dry soil before subsequent mixing with distilled water. Thus, this mixing procedure was adopted in this research program.

A summary of all tested samples after the above-mentioned mixing procedure is presented in Table 3. Within this table, the following abbreviations are used: S for natural soil; W_BS for reinforced soil with wollastonite microfibres based on different percentages (B) of microfibres and different curing times (T); $S_{(200,24)}$ for carbonated natural soil at 200 kPa pressure and after 24 h; $C_{(P,T)}SW_B$ for carbonated reinforced soil at different CO_2 pressures (P) and different curing periods (T).

The quantity of water at the time of mixing corresponded to the optimum moisture content of the original soil and of the W_BS mixture (Table 3), which were both determined by standard Proctor compaction tests (BS 1377-1990 (BSI, 1990)).

2.2.2. *Carbonation set up*

Figure 1 shows the triaxial cell used to infuse pressurised gaseous CO_2 throughout the original and reinforced soil samples, which were previously subjected to a confining pressure of 400 kPa, followed by the upward forced permeation of the CO_2. The outflow tube was placed

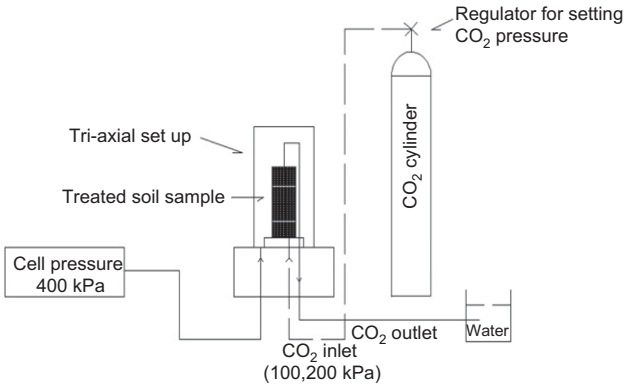

Figure 1. Triaxial setup for carbonation of reinforced-soil samples used in this research

under water to detect whether or not the samples were fully saturated with CO_2 gas. After a few minutes, the outflow tap was closed while the inlet was kept open. Since the CO_2 mineralisation of materials such as wollastonite and olivine is significantly influenced by CO_2 exposure time and pressure, the samples were carbonated at CO_2 pressures of 100 and 200 kPa, over periods of 7, 48 and 168 h.

2.2.3. *Unconfined compressive strength test*

The specimens used for the uniaxial compression strength (UCS) tests were prepared directly after the above-mentioned mixing procedure, by manual compaction, in a cylindrical mould 50 mm in diameter and 100 mm in height. A 45 mm diameter steel rod was used to apply a static load in three similar layers. The specimens were extruded and immediately wrapped in plastic sheets and polythene covers to prevent moisture loss (Table 3). To achieve a state of approximate saturation before the UCS tests, the specimens were unwrapped and submerged in water for the last 24 h of their respective curing periods. This saturation eliminates the positive effects of suction on the specimens' compressive strength (Pourakbar *et al.* 2015a, 2015b, 2016; Pourakbar and Huat 2017). The exception to this saturation procedure was the original soil specimens (S), which would lose structural integrity if submerged.

The UCS measurement was conducted in accordance with Part 7: Clause 7 of BS 1377 (1990). UCS values were

measured in three different specimens, and the results reported had a deviation from the average value of less than 5%. An Instron 3366 universal testing machine was used, fitted with a 100 kN load cell, and the tests were carried out under monotonic displacement control, at a rate of 0.2 mm/min, and the entire stress-strain curve was obtained from each test.

2.2.4. *Flexural strength test*

The flexural strength test (FS) specimens were identical to the UCS specimens, and cured under exactly the same conditions. A three-point bending test over a support span of 60 mm was then performed, according to ASTM D1635, under a monotonic speed of 0.1 mm/min. The flexural stress for the circular section of the outer layer of the specimen was calculated using (Equation 5)

$$f = \frac{PrL}{\pi r^3} \tag{5}$$

where Pr is the maximal applied load, r is the radius of the specimen and L is the distance between the supports.

2.2.5. *Indirect tensile strength test*

The characteristic tensile strength of a soil mass is an important property when designing structures such as earth dams or pavement foundations. Tensile stresses are attributed to factors including wheels rolling on a pavement, shrinkage of soil, seasonal variations in temperature, and moisture changes (wet-dry cycles) for example. Various tests have been developed and conducted to determine the tensile strength of stabilised soils (Kumar and Gupta 2016), such as the direct tensile test, the 3-point bending test, the double punch tensile test, indirect tensile strength test and the split cylinder test. The indirect tensile test (ITS) was adopted in this study due to its simplicity and suitability. It was conducted based on ASTM D3379, as well as other relevant literature detailing this experimental procedure, either in soils (Dexter and Kroesbergen 1985; Pourakbar *et al.* 2016; Cristelo *et al.* 2017) or rock (Yu *et al.* 2006) specimens. For this study, cylindrical specimens 100 mm in length and 50 mm in diameter were used, with similar curing conditions to those described for the UCS specimens. After 28 days' curing, the ITS tests were conducted by applying the load, at a rate of 0.1 mm/min, on opposite surfaces of the specimen.

2.2.6. *Microstructural analysis*

To better understand the effect of incorporating the reinforcement, as well as the micro-changes promoted by carbonation, representative fragments of the reinforced soil, collected after the mechanical tests, were analysed using scanning electron microscopy (SEM), energy dispersive X-ray spectroscopy (EDS) and X-ray diffraction (XRD). For the SEM/EDS analysis, the fragments were mounted on aluminium stubs with double-sided carbon tabs, and then sputter coated with a thin layer of platinum. The XRD was performed using a Bruker D8 ADVANCE X-ray diffractometer, using CuK_α radiation (at 40 kV and 40 mA emission current), equipped with a graphite monochromator and a NaI scintillation detector.

3. RESULTS AND DISCUSSION

3.1. Compressive strength of the reinforced soil before and after carbonation

Figure 2 shows the stress-strain behaviour of the reinforced soil after curing times of 7, 14 and 28 days. As can be seen, the inclusion of microfibre into the soil matrix induced a slight increase in strength. For the $W_{15\%}S$ and $W_{20\%}S$ mixtures, and after 28 days of curing, values of 422 and 587 kPa were observed, respectively. Moreover, compared to the untreated soil (S), the presence of microfibres (W_BS group) dramatically modified the stress–strain behaviour of the mixtures, especially at very

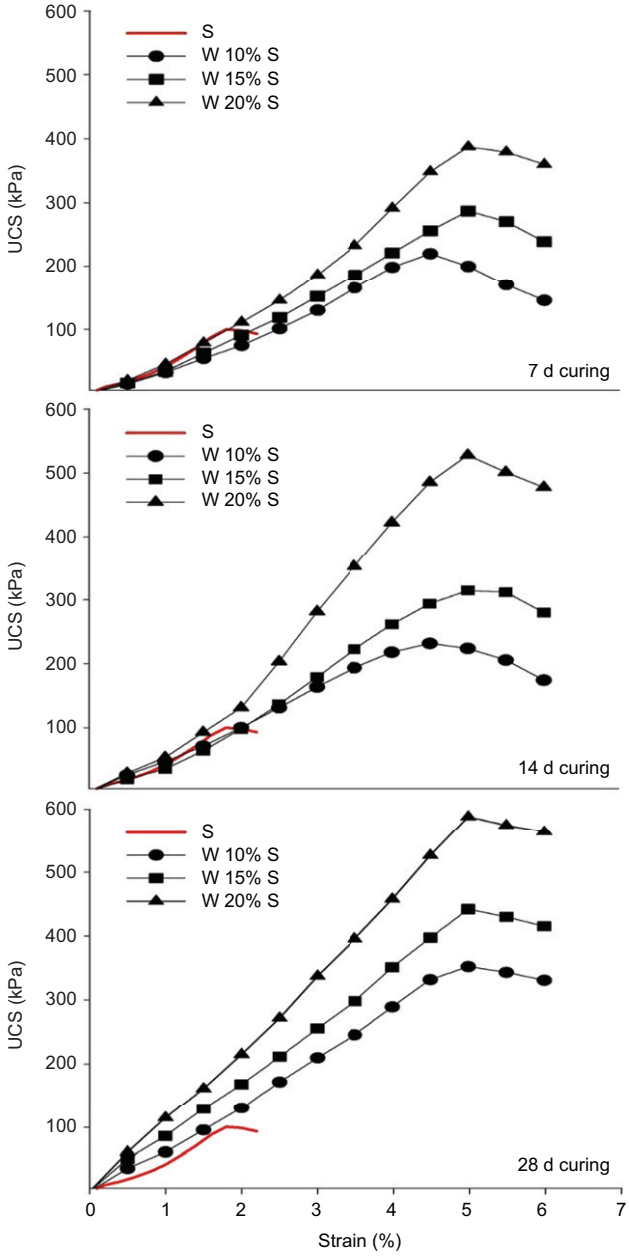

Figure 2. Stress-strain behaviour of reinforced soil samples before carbonation after 7, 14, and 28 day curing

large strains. Thus, as a general tendency, and regardless of curing time, the use of microfibres alone in the soil matrix increased the strain behaviour of soil specimens. Furthermore, the strain at failure increased with increasing fibre content, which denoted a significant behavioural transformation from brittle to ductile. The addition of 15% wollastonite microfibres ($W_{15\%}S$) was sufficient to ensure a strain hardening behaviour.

According to previous research developed by the authors (Pourakbar *et al.* 2016; Pourakbar and Huat 2017), the slight increase in strength with increasing fibre content is due to the increasing contact area between the fibre and the surrounding soil particles. Since the particle-fibre interface possesses considerable friction, it becomes increasingly more difficult for the soil particles to experience relative position changes.

Although the time period between the fabrication and testing of the specimens showed an increase in strength, this was not considered significant since no substantial chemical reactions are expected to occur during this period. Instead, the strength increase was attributed to the reduction in moisture content of the fibre-reinforced soil samples (W_BS group) after extended curing times (in excess of 28 days) at ambient temperature. The slight increase in the UCS values was thus attributed to the reduction in the lubricating effect of the moisture, which slightly increased the load transferred between the fibres and the soil grains. However, it was observed that the maximum shear strength of the W_BS group was limited to only 587 kPa (after 28 days).

The stress-strain behaviour after carbonation of the mixtures containing 20% fibres is presented in Figure 3, considering different pressures and carbonation periods. The figure shows that carbonation of reinforced soil results in a sharp and rapid strength increase, which is, nevertheless, a function of the carbon dioxide pressure and carbonation period. For the same period of carbonation, a rapid strength increase was observed when the CO_2 pressure increased from 100 kPa to 200 kPa. According to previous researches (Fasihnikoutalab *et al.* 2016a, 2016b, 2017a), the degree of strength gain with increasing CO_2 pressure depends on the calcium or magnesium content of the blend. Therefore, greater UCS increases can be predicted with longer carbonation periods, at least while all the Ca content of the fibres (about 40–50%, see Table 2) is not consumed. This was confirmed by the fact that an increase in CO_2 pressure results in a greater amount of Ca^{2+} ions participating in the carbonation reactions, according with Equation 4 (De Silva *et al.* 2009; Mo and Panesar 2012).

3.2. Indirect tensile strength of the reinforced soil before and after carbonation

The tensile stress-deflection curves of the original and fibre-reinforced soil, after curing for 28 days and after carbonation, are shown in Figure 4. It can be seen that the increase in fibre content not only promoted an increase in peak stress and an increase in the deflection at peak stress, but it also promoted a significant change in the post-peak behaviour. Compared to the natural soil (S), the ITS of the $W_{15\%}S$ and $W_{20\%}S$ specimens increased by 400% and 638%, respectively. These results are consistent with those obtained by other researchers (Fatahi *et al.* 2012; Correia *et al.* 2015; Cristelo *et al.* 2017) who assessed the indirect tensile response of artificially cemented soils reinforced

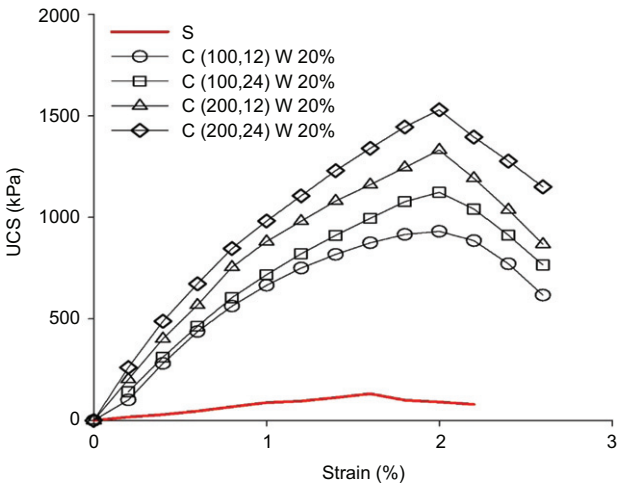

Figure 3. Stress-strain behaviour of carbonated reinforced soil samples

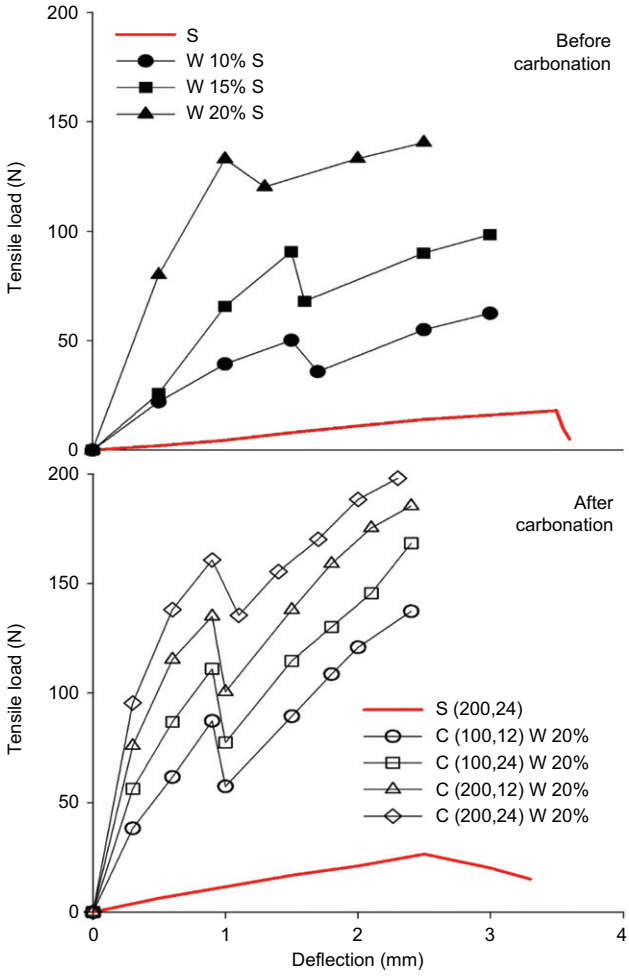

Figure 4. Tensile load-deflection of reinforced samples cured for 28 days and after carbonation

with polypropylene fibres. They reported a sharp increase in the ITS peak value in addition to substantial modifications in the post-peak behaviour. This improvement in the post-peak behaviour of the W_BS group is commonly attributed to the 'bridge' effect established by the fibres embedded in the soil matrix, as reported by Tang *et al*. (2007). The fibres are thus capable of reducing further development of tension cracks during the loading process and, consequently, the deformation of the soil.

After carbonation, the ITS of the $W_{20\%}S$ mixture increased by 38 times, and after carbonation ($S_{(200,24)}$) increased by 45 times relative to the natural soil. Based on this result, it is possible to conclude that the carbonation is only effective when the fibres are also added to the soil. Also worth mentioning is the fact that the carbonation reduced the maximum tensile load, while also increasing the deflection at peak load. This might be explained by the modifications, induced by the carbonation, to the wollastonite mineral of the fibres. Indeed, the Ca recovered from the fibres favours the formation of a binder inside the soil voids, but it depletes the fibres of some of their load-bearing capacity. This effect is not significant in terms of compression loading (in this case, carbonation had a clearly positive effect over the fibre-reinforced specimens), since the tensile strength of the fibres is, in this case, of lower importance, but it does pose a significant question mark over the use of carbonation when tensile strength is expected to be governing the overall performance of the fibre-reinforced soil.

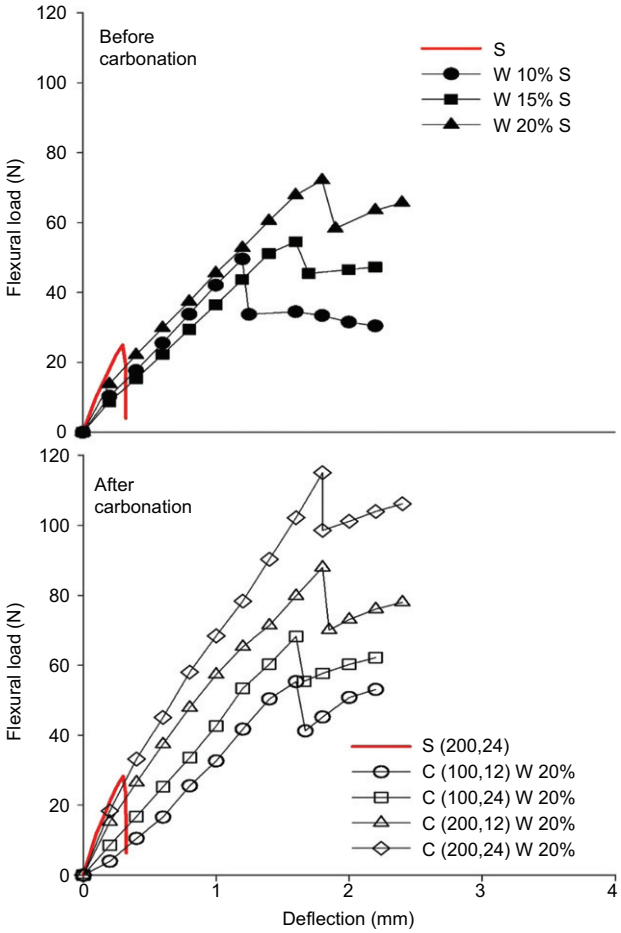

Figure 5. Flexure load-deflection of reinforced samples cured for 28 days and after carbonation

3.3. Flexural strength of the reinforced soil before and after carbonation

The flexural load-deflection curves of the reinforced samples, after 28 days curing time and after carbonation, are shown in Figure 5. The clear peak observed in each curve is a direct measure of the flexural stress (FS) of the specimens. A significant increase in the peak FS was observed with the addition of fibres (W_BS group), together with an increase in the corresponding deflection. The FS of the $W_{20\%}S$ mixture was 85 kPa, which was 183% higher than the FS of the natural soil (30 kPa). The addition of fibres was beneficial, when comparing the natural soil strength with the 20% fibre mixture and $C_{(200,24)}W_{20\%}$, exhibiting a strength improvement of 306%.

However, the fibre reinforcement did not affect the initial stiffness. Additionally, and for every mixture tested, the load-deflection curve showed a deviation in linearity, which is attributed to the development of damage in the section under maximum flexural moment. Such damage is characterised by the formation of a fracture process zone (FPZ), which assumes non-negligible dimensions for quasi-brittle materials, especially when compared with the specimen size. Also relevant is the modification from a fragile to a quasi-fragile behaviour, attributed to the addition of fibres, which was detected through the post-peak segment of the load-deflection curves. This indicates that, although slight, there was indeed an increase in toughness due to the fibres' inclusion in all the mixtures (uncarbonated and carbonated cases).

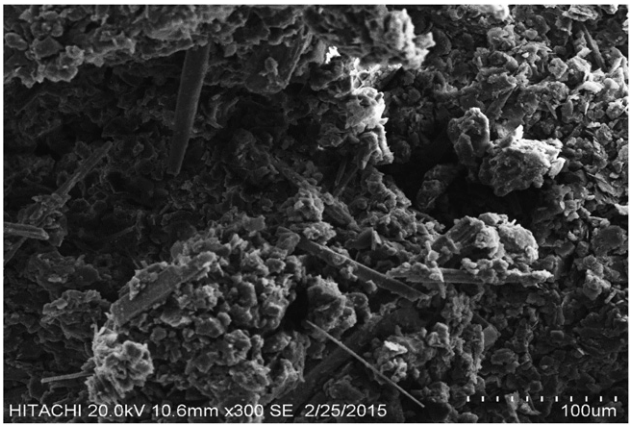

Figure 6. SEM image of $W_{20\%}S$

3.4. Microstructural analysis

3.4.1. *SEM and EDS analysis*

Figure 6 illustrates how the shape of the microfibres is ideally suited to soil reinforcement, through bridging between the soil particles. Figure 7 shows the SEM image of $W_{20\%}$ after 28 days' curing time and $C_{(200,24)}W_{20\%}$ respectively. This allows the soil particles to be locked in their original positions after 28 days curing time and after carbonation, resulting in an improvement in the

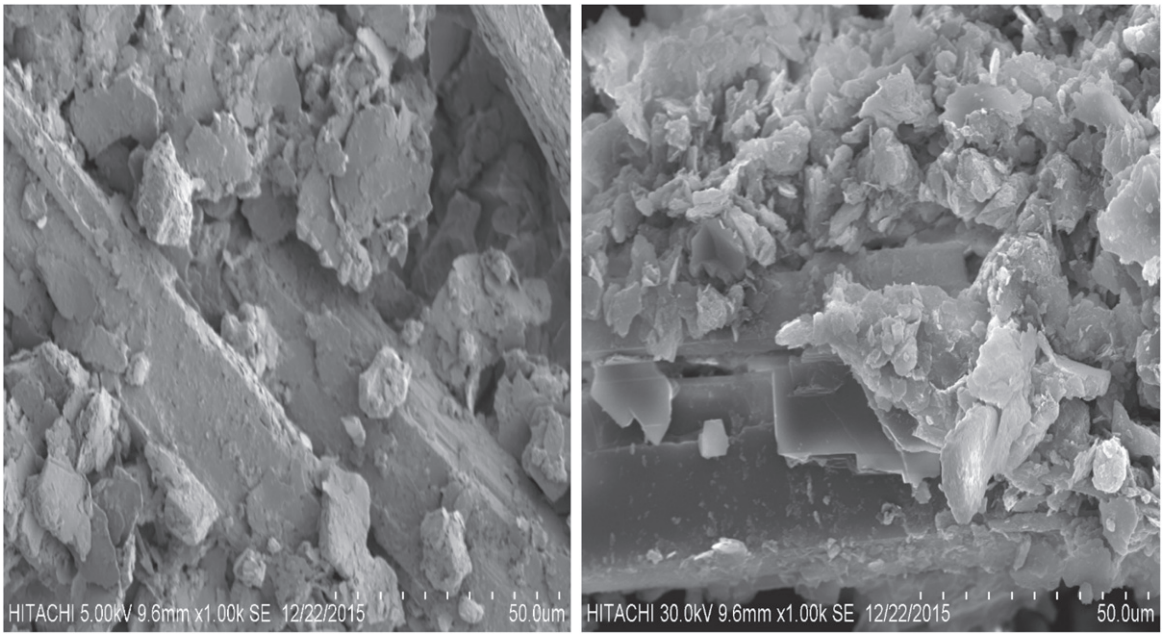

Figure 7. SEM image of (a) $W_{20\%}$ after 28 days' curing time and (b) $C_{(200,24)}W_{20\%}$ specimen after carbonation

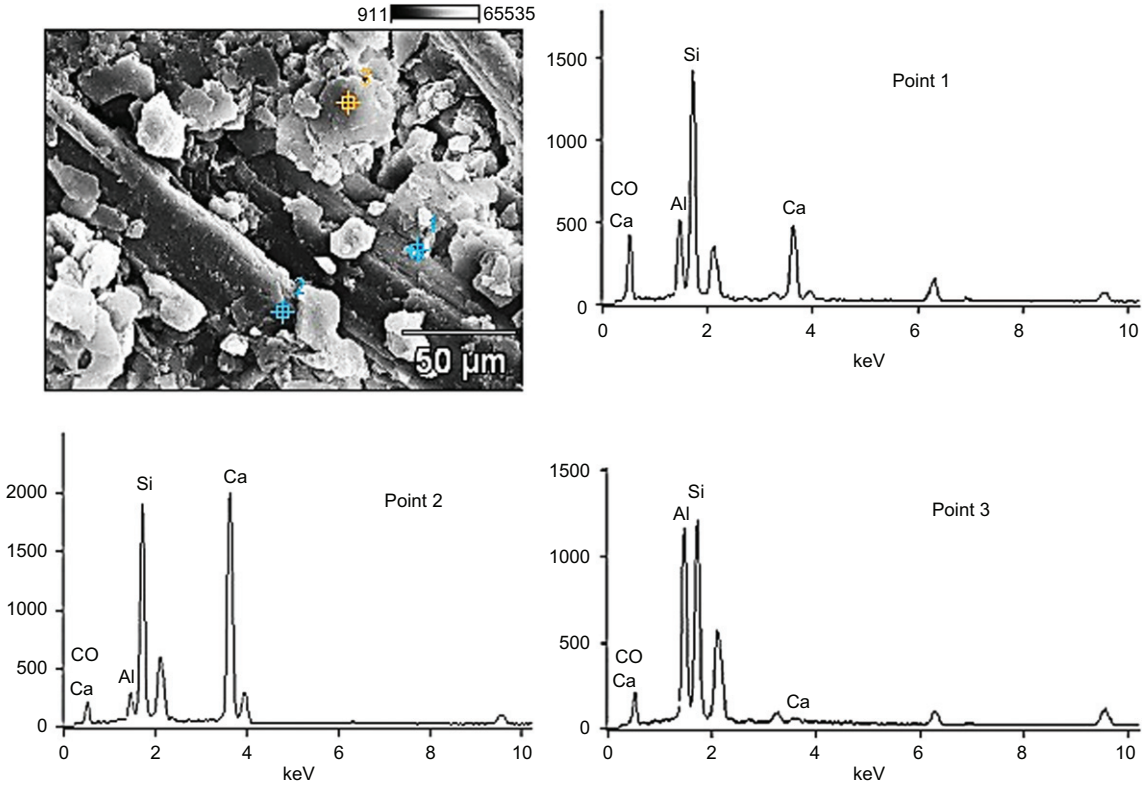

Components	C	O	Al	Si	Ca
Point 1	4.85	44.73S	9.68	35.76	4.99
Point 2	2.68	47.33S	2.58	32.38	13.08
Point 3	3.15	38.86S	23.28	34.11	7.36

Figure 8. EDS analysis of a $W_{20\%}S$ after 28 days' curing and corresponding table showing composition in weight percent

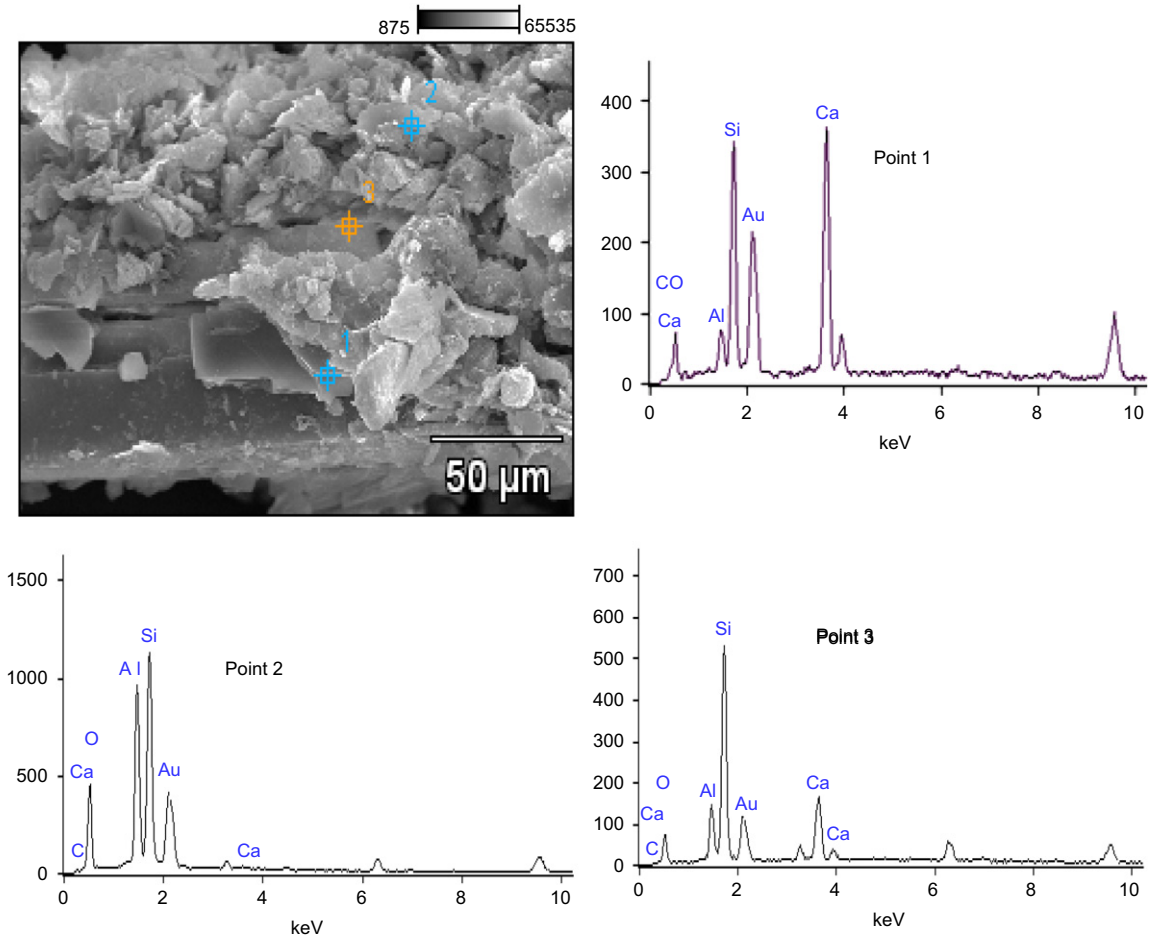

Components	C	O	Al	Si	Ca
Point 1	2.69	45.28	4.85	30.04	13.85
Point 2	3.89	39.32	21.75	34.51	9.1
Point 3	3.75	47.87	8.08	37.22	6.83

Figure 9. EDS analysis of a $C_{(200,24)}W_{20\%}$ specimen after carbonation and corresponding table showing composition in weight percent

mechanical properties including post-peak strength, ductility, tensile, and flexural strength, as illustrated in Figures 2, 4a and 5a.

Figure 8 shows an EDS analysis of a specimen with 20% microfibres ($W_{20\%}S$) after 28 days. The high amounts of Ca and O elements are attributed to the leaching of wollastonite, described in Equation 2, which produced calcium-silicate-hydrate (C–S–H) gel between the soil particles (Huijgen *et al*. 2006). This may be a key stage in the process of soil improvement using this type of microfibre.

Figure 9 show the EDS analysis of $C_{(200,24)}W_{20\%}$, when subsequently exposed to CO_2 at pressures of 200 kPa. The EDS clearly shows how carbonation of the microfibre affected the elements compared to Figure 8.

3.4.2. *XRD analysis*

Figure 10 shows the XRD diffractograms of the natural soil, the wollastonite fibres, the W20%S mixture (after 28 days) and the $C_{(200,48)}$W20% mixture. The soil mineralogy shows the presence of quartz and kaolinite. The main crystalline phase in the microfibres is CaO, while amorphous SiO_2 was also detected. The $W_{20\%}S$ mixture included crystalline SiO_2 (from the soil) and CaO (from the wollastonite).

The XRD analysis of the 20% wollastonite microfibre-treated soil, after 28 days' curing, and after carbonation revealed the presence of additional peaks assigned to SiO_2 and $CaCO_3$ phases.

4. CONCLUSIONS

- Compared to untreated soil (S), the presence of microfibres at quantities up to 20% (W_BS group) modified the stress–strain behaviour of the mixture at very large strains. In this respect, the inclusion of microfibres in the soil matrix induced an increase in strength. For the $W_{15\%}S$ and $W_{20\%}S$ mixtures, and after 28 days of curing, values of

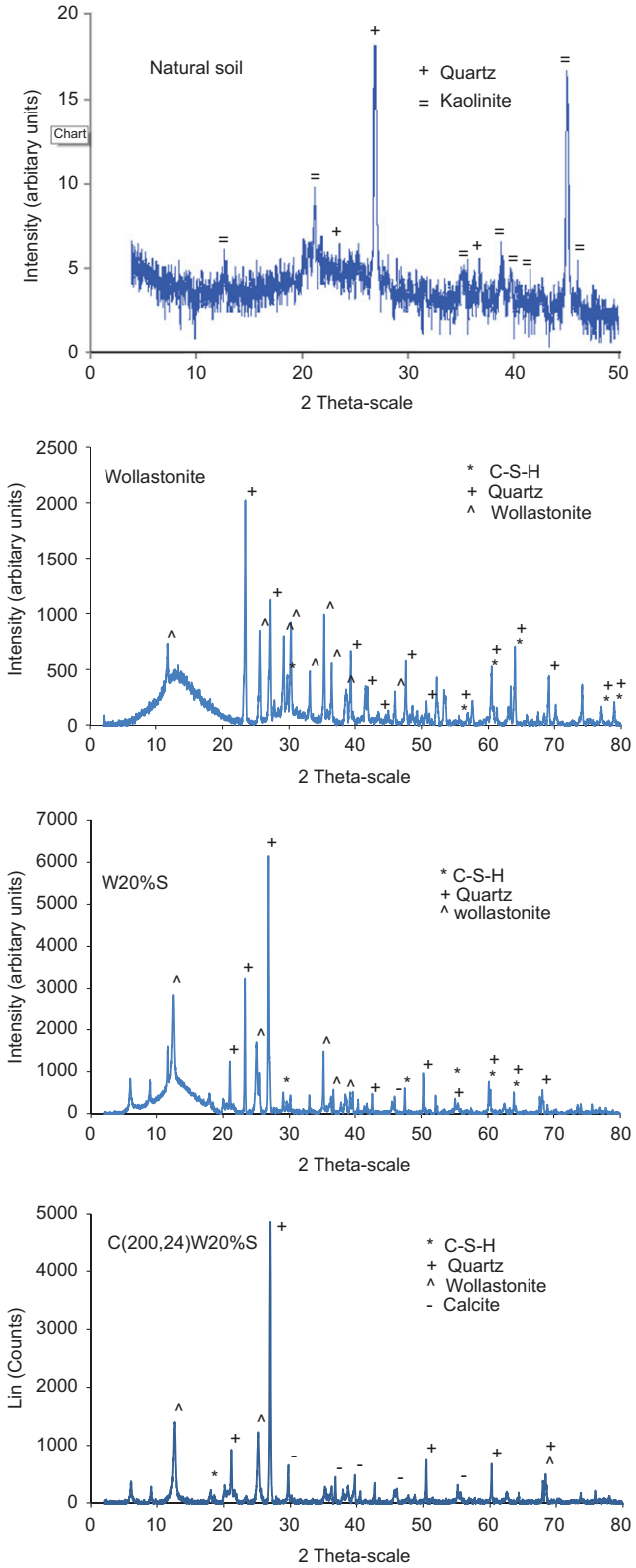

Figure 10. XRD analysis of natural soil, natural wollastonite, $W_{20\%}S$ after 28 days and $C_{(200,24)}W_{20\%}$

422 and 587 kPa were observed, respectively. Besides, failure strain increased in line with increasing fibre content, which denoted a significant transformation from brittle to ductile behaviour. The slight increase in the UCS values may be attributed to the reduction in the effect of water lubrication and increase in bonding between soil particles during shear.

- Unconfined compressive values confirmed that carbonation of reinforced soil results in a sharp and rapid strength increase depending on carbon dioxide pressure and carbonation period. In this regard, a rapid strength increase was observed, when the CO_2 pressure increased from 100 kPa to 200 kPa. Together with the increase in UCS values, a brittle behaviour was also noted in the case of reinforced samples following carbonation.
- According to the flexural strength and ITS tests, a significant increase in the peak flexural load and ITS values with the addition of fibres (W_BS group) was observed. Also, the ITS values and flexural load performance of reinforced soil improved with the carbonation process.
- The SEM images showed how the wollastonite microfibres react with soil after 28 days' curing time and after carbonation.
- EDS results confirmed that an increase in the two major elements (Ca and O) detected is attributed to the leaching of wollastonite microfibres. This may be a key stage in the process of soil improvement attributed to microfibre and soil particle interactions before and after the carbonation process.
- The XRD analysis proved that carbonation affected the phase composition of the wollastonite microfibre-treated soils exposed to different treatments.

NOTATION

Basic SI units are given in parentheses.

f	Flexural stress (Pa)
FS	Flexural strength (Pa)
L	distance between the supports for flexural test (m)
MDD	Maximum dry density (kg/m^3)
OMC	Optimum moisture content (dimensionless)
P	Pressure (Pa)
Pr	maximal applied load
r	Radius of the specimen (m)
T	Curing time (s)
UCS	Unconfined compressive strength (Pa)

ABBREVIATIONS

$C_{(P,T)}SW_B$	Carbonated reinforced-soil at different CO_2 pressures
C–A–H	Calcium aluminium hydrate
C–S–H	Calcium silicate hydrate
EDS	Energy dispersive X-ray spectroscopy
ITS	Indirect tensile strength
S	Natural soil
$S_{(200,24)}$	Carbonated natural soil at 200 kPa pressure
SEM	Scanning electron microscopy
W_BS	Reinforced soil with wollastonite microfibres
XRD	X-ray diffraction
XRF	X-ray fluorescence

REFERENCES

Aggarwal, P. & Sharma, B. (2011). Application of jute fiber in the improvement of subgrade characteristics. *ACEE International Journal on Transportation and Urban Development*, **1**, No. 1, 27–30.

Andreani, M., Luquot, L., Gouze, P., Godard, M., Hoise, E. & Gibert, B. (2009). Experimental study of carbon sequestration reactions controlled by the percolation of CO_2-rich brine through peridotites. *Environmental Science & Technology*, **43**, No. 4, 1226–1231.

Ashraf, W., Olek, J. & Tian, N. (2016). Multiscale characterization of carbonated wollastonite paste and application of homogenization schemes to predict its effective elastic modulus. *Cement and Concrete Composites*, **27**, 284–298.

ASTM D1635 *Standard Test Method for Flexural Strength of Soil Cement using Simple Beam with Three Point Loading*. ASTM International, West Conshohocken, PA, USA.

ASTM D3379 *Standard Test Method for Tensile Strength and Young's Modulus for High-Modulus Single-Filament Materials*. ASTM International, West Conshohocken, PA, USA.

ASTM D2487 *Standard Practice for Classification of Soils for Engineering Purposes (Unified Soil Classification System)*. ASTM International, West Conshohocken, PA, USA.

Botero, E., Ossa, A., Sherwell, G. & Ovando-Shelley, E. (2015). Stress–strain behavior of a silty soil reinforced with polyethylene terephthalate (PET). *Geotextiles and Geomembranes*, **43**, No. 4, 363–369.

BSI (1990). *BS1377: Methods of test for soils and civil engineering purposes*. BSI, London, UK.

Clark, J. (1998). *Future of Automotive Body Materials, Steel, Aluminum and Polymer Composites*, Hoogovens Technology, Massachusetts Institute of Technology, Cambridge, MA, USA.

Consoli, N., Corte, M. B. & Festugato, L. (2012). Key parameter for tensile and compressive strength of fibre-reinforced soil–lime mixtures. *Geosynthetics International*, **19**, No. 5, 409–414.

Correia, A. A., Oliveira, P. J. V. & Custódio, D. G. (2015). Effect of polypropylene fibres on the compressive and tensile strength of a soft soil, artificially stabilised with binders. *Geotextiles and Geomembranes*, **43**, No. 2, 97–106.

Cristelo, N., Cunha, V. M., Dias, M., Gomes, A. T., Miranda, T. & Araújo, N. (2015). Influence of discrete fibre reinforcement on the uniaxial compression response and seismic wave velocity of a cement-stabilised sandy-clay. *Geotextiles and Geomembranes*, **43**, No. 1, 1–13.

Cristelo, N., Cunha, V. M., Gomes, A. T., Araújo, N., Miranda, T. & De Lurdes Lopes, M. (2017). Influence of fibre reinforcement on the post-cracking behaviour of a cement-stabilised sandy-clay subjected to indirect tensile stress. *Construction and Building Materials*, **138**, 163–173.

Daval, D., Martinez, I., Guigner, J. M., Hellmann, R., Corvisier, J., Findling, N., Dominici, C., Goffé, B. & Guyot, F. (2009). Mechanism of wollastonite carbonation deduced from micro-to nanometer length scale observations. *American Mineralogist*, **94**, No. 11–12, 1707–1726.

Dexter, A. & Kroesbergen, B. (1985). Methodology for determination of tensile strength of soil aggregates. *Journal of Agricultural Engineering Research*, **31**, No. 2, 139–147.

Dey, V., Kachala, R., Bonakdar, A. & Mobasher, B. (2015). Mechanical properties of micro and sub-micron wollastonite fibers in cementitious composites. *Construction and Building Materials*, **82**, 351–359.

Ding, L., Ma, L., Luo, H., Yu, M. & Wu, X. (2011). Wavelet analysis for tunneling-induced ground settlement based on a stochastic model. *Tunnelling and Underground Space Technology*, **26**, No. 5, 619–628.

Estabragh, A., Namdar, P. & Javadi, A. (2012). Behavior of cement-stabilized clay reinforced with nylon fiber. *Geosynthetics International*, **19**, No. 1, 85–92.

Fasihnikoutalab, M. H. (2015). Olivine for soil stabilization. *Pertanika Journal of Scholarly Research Reviews*, **1**, No. 1, 18–26.

Fasihnikoutalab, M. H., Asadi, A., Huat, B. K., Ball, R. J., Pourakbar, S. & Singh, P. (2016a). Utilisation of carbonating olivine for sustainable soil stabilisation. *Environmental Geotechnics*, **4**, No. 3, 184–198.

Fasihnikoutalab, M. H., Asadi, A., Huat, B. K., Westgate, P., Ball, R. J. & Pourakbar, S. (2016b). Laboratory-scale model of carbon dioxide deposition for soil stabilisation. *Journal of Rock Mechanics and Geotechnical Engineering*, **8**, No. 2, 178–186.

Fasihnikoutalab, M. H., Asadi, A., Unluer, C., Huat, B. K., Ball, R. J. & Pourakbar, S. (2017a). Utilization of alkali-activated olivine in soil stabilization and the effect of carbonation on unconfined compressive strength and microstructure. *Journal of Materials in Civil Engineering*, **29**, No. 6, 601–613.

Fasihnikoutalab, M. H., Pourakbar, S., Ball, R. J. & Huat, B. K. (2017b). The effect of olivine content and curing time on the strength of treated soil in presence of potassium hydroxide. *International Journal of Geosynthetics and Ground Engineering*, **3**, No. 2, 1–10.

Fatahi, B., Khabbaz, H. & Fatahi, B. (2012). Mechanical characteristics of soft clay treated with fibre and cement. *Geosynthetics International*, **19**, No. 3, 252–262.

Güllü, H. & Khudir, A. (2014). Effect of freeze–thaw cycles on unconfined compressive strength of fine-grained soil treated with jute fiber, steel fiber and lime. *Cold Regions Science and Technology*, **106**, 55–65.

Hejazi, S. M., Sheikhzadeh, M., Abtahi, S. M. & Zadhoush, A. (2012). A simple review of soil reinforcement by using natural and synthetic fibers. *Construction and Building Materials*, **30**, 100–116.

Huijgen, W. J., Witkamp, G. J. & Comans, R. N. (2006). Mechanisms of aqueous wollastonite carbonation as a possible CO_2 sequestration process. *Chemical Engineering Science*, **61**, No. 13, 4242–4251.

Kalla, P., Misra, A., Gupta, R. C., Csetenyi, L., Gahlot, V. & Arora, A. (2013). Mechanical and durability studies on concrete containing wollastonite–fly ash combination. *Construction and Building Materials*, **40**, 1142–1150.

Kumar, A. & Gupta, D. (2016). Behavior of cement-stabilized fiber-reinforced pond ash, rice husk ash–soil mixtures. *Geotextiles and Geomembranes*, **44**, No. 3, 466–474.

Lackner, K. S., Butt, D. P. & Wendt, C. H. (1997). Progress on binding CO_2 in mineral substrates. *Energy Conversion and Management*, **38**, S259–S264.

Lin, T., Jia, D., He, P. & Wang, M. (2010). In situ crack growth observation and fracture behavior of short carbon fiber reinforced geopolymer matrix composites. *Materials Science and Engineering*, **527**, No. 9, 2404–2407.

Low, N. M. & Beaudoin, J. J. (1993). The effect of wollastonite micro-fibre aspect ratio on reinforcement of Portland cement-based binders. *Cement and Concrete Research*, **23**, No. 6, 1467–1479.

Low, N. M. & Beaudoin, J. J. (1994a). The flexural toughness and ductility of Portland cement-based binders reinforced with wollastonite micro-fibres. *Cement and Concrete Research*, **24**, No. 2, 250–258.

Low, N. M. & Beaudoin, J. (1994b). Stability of Portland cement-based binders reinforced with natural wollastonite micro-fibres. *Cement and Concrete Research*, **24**, No. 5, 874–884.

Maliakal, T. & Thiyyakkandi, S. (2013). Influence of randomly distributed coir fibers on shear strength of clay. *Geotechnical and Geological Engineering*, **31**, No. 2, 425–433.

Marandi, S., Bagheripour, M., Rahgozar, R. & Zare, H. (2008). Strength and ductility of randomly distributed palm fibers reinforced silty-sand soils. *American Journal of Applied Sciences*, **5**, No. 3, 209–216.

Mirzababaei, M., Miraftab, M., Mohamed, M. & Mcmahon, P. (2012). Unconfined compression strength of reinforced clays with carpet waste fibers. *Journal of Geotechnical and Geoenvironmental Engineering*, **139**, No. 3, 483–493.

O'Connor, W., Dahlin, D., Rush, G., Gerdemann, S., Penner, L. & Nilsen, D. (2005). *Aqueous Mineral Carbonation*, Final Report. Department of Energy ARC-TR-04-002, Washington, USA.

Pourakbar, S. & Huat, B. K. (2016). A review of alternatives traditional cementitious binders for engineering improvement of soils. *International Journal of Geotechnical Engineering*, **11**, No. 2, 1–11.

Pourakbar, S. & Huat, B. (2017). Laboratory-scale model of reinforced alkali-activated agro-waste for clayey soil stabilization. *Advances in Civil Engineering Materials*, **6**, No. 1, 83–105.

Pourakbar, S., Asadi, A., Huat, B. B. & Fasihnikoutalab, M. H. (2015a). Stabilization of clayey soil using ultrafine palm oil fuel ash (POFA) and cement. *Transportation Geotechnics*, **3**, 24–35.

Pourakbar, S., Asadi, A., Huat, B. B. & Fasihnikoutalab, M. H. (2015b). Soil stabilization with alkali-activated agro-waste. *Environmental Geotechnics*, **2**, No. 6, 359–370.

Pourakbar, S., Asadi, A., Huat, B. B., Cristelo, N. & Fasihnikoutalab, M. H. (2016). Application of alkali-activated agro-waste reinforced with wollastonite fibers in soil stabilization. *Journal of Materials in Civil Engineering*, **29**, No. 2, 401–413.

Prabakar, J. & Sridhar, R. (2002). Effect of random inclusion of sisal fibre on strength behaviour of soil. *Construction and Building Materials*, **16**, No. 2, 123–131.

Prigiobbe, V., Hänchen, M., Werner, M., Baciocchi, R. & Mazzotti, M. (2009). Mineral carbonation process for CO_2 sequestration. *Energy Procedia*, **1**, No. 1, 4885–4890.

Ramesh, H., Krishna, K. M. & Mamatha, H. (2010). Compaction and strength behavior of lime-coir fiber treated Black Cotton soil. *Geomechanic Engineering*, **2**, No. 1, 19–28.

Saltevskaya, L., Livson, Z. & Ryshchenko, M. (1974). Synthesis of wollastonite and its use in ceramic bodies. *Glass and Ceramics*, **31**, No. 2, 114–117.

Singh, H. & Bagra, M. (2013). Improvement in CBR value of soil reinforced with Jute Fiber. *International Journal of Innovative Research in Science, Engineering and Technology*, **2**, No. 8, 3447–3452.

Sivakumar Babu, G. & Vasudevan, A. (2008). Strength and stiffness response of coir fiber-reinforced tropical soil. *Journal of Materials in Civil Engineering*, **20**, No. 9, 571–577.

Soliman, A. & Nehdi, M. (2011). Effect of natural wollastonite microfibers on early-age behavior of UHPC. *Journal of Materials in Civil Engineering*, **24**, No. 7, 816–824.

Sukontasukkul, P. & Jamsawang, P. (2012). Use of steel and polypropylene fibers to improve flexural performance of deep soil–cement column. *Construction and Building Materials*, **29**, 201–205.

Tai, C. Y., Chen, W. R. & Shih, S. M. (2006). Factors affecting wollastonite carbonation under CO_2 supercritical conditions. *AIChE Journal*, **52**, No. 1, 292–299.

Tang, C., Shi, B., Gao, W., Chen, F. & Cai, Y. (2007). Strength and mechanical behavior of short polypropylene fiber reinforced and cement stabilized clayey soil. *Geotextiles and Geomembranes*, **25**, No. 3, 194–202.

Thwe, M. M. & Liao, K. (2002). Effects of environmental aging on the mechanical properties of bamboo–glass fiber reinforced polymer matrix hybrid composites. *Composites Part A, Applied Science and Manufacturing*, **33**, No. 1, 43–52.

Yeung, A. T., Cheng, Y., Tham, L., Au, A. S., So, S. T. & Choi, Y. K. (2007). Field evaluation of a glass-fiber soil reinforcement system. *Journal of Performance of Constructed Facilities*, **21**, No. 1, 26–34.

Yu, Y., Yin, J. & Zhong, Z. (2006). Shape effects in the Brazilian tensile strength test and a 3D FEM correction. *International Journal of Rock Mechanics and Mining Sciences*, **43**, No. 4, 623–627.

Zhao, L., Sang, L., Chen, J., Ji, J. & Teng, H. H. (2009). Aqueous carbonation of natural brucite, relevance to CO_2 sequestration. *Environmental Science & Technology*, **44**, No. 1, 406–411.

The Editor welcomes discussion on all papers published in Geosynthetics International. Please email your contribution to discussion@geosynthetics-international.com by 15 June 2018.